Synthesis and study of the protective properties of the product of the reaction of glyoxal, ammonia, and acetaldehyde against hydrogen sulfide corrosion of carbon steel in model stratum waters

A.E. Abramov, A.A. Uryadnikov, T.V. Semenyuk and L.E. Tsygankova*

Derzhavin State University, ul. Internatsyonalnaya, 33, 392000 Tambov, Russian Federation
**E-mail: vits21@mail.ru*

Abstract

The G. Debus–B.L. Radzishevsky reaction with participation of glyoxal, ammonia, and acetaldehyde made it possible to obtain a product exhibiting inhibitory activity. The composition of the product was analyzed by IR spectroscopy and chromato-mass spectrometry. The inhibitory activity is due to the presence of nitrogen-containing substances, including imidazole and its derivatives. The corrosion inhibitory effect was studied against carbon steel corrosion in NACE and M1 model stratum waters saturated with H_2S. The study was carried out by the gravimetry, potentiodynamic polarization and impedance spectroscopy methods. According to gravimetry, the protective effect (Z) of the product at a concentration of 200 mg/L is about 60% in the NACE medium and 70% in M1 medium containing 400 mg/L H_2S at an experiment duration of 24 hours. Polarization measurements show higher Z values equal to 83% and 98%, respectively. The deceleration of corrosion is due to the inhibition of both partial electrode reactions in the NACE medium and the anodic reaction in the M1 solution due to the adsorption of the product components on the metal in accordance with the Langmuir isotherm. The calculated value of the free energy of adsorption equal to 28.5 kJ/mol indicates the physical adsorption of inhibitory components with a certain amount of chemisorption.

Keywords: *imidazole derivatives, inhibitor, steel, corrosion, inhibition, hydrogen sulfide, gravimetry, polarization, impedance.*

Received: January 12, 2023. Published: February 8, 2023 doi: 10.17675/2305-6894-2023-12-1-8

Introduction

The use of inhibitors is one of the most common methods for protecting metals against corrosion in various environments. Organic compounds containing oxygen, sulfur, nitrogen, phosphorus, and multiple bonds have become widespread as inhibitors. It is presence of these elements that promotes the adsorption of such compounds on the metal surface with the formation of a protective coating. Among them, imidazole derivatives are known, which, due to the presence of π-electrons in the −C=N azomethine double bond, are able to coordinate with metals, forming a barrier between them and a corrosive environment. In

addition, they are characterized by low cost and ease of synthesis. Their protective properties with respect to zinc, brass and copper in alkaline and neutral media are known [1]. Imidazole derivatives are corrosion inhibitors for copper in solutions of sulfuric, hydrochloric, and nitric acids [2–5] and for aluminum in HCl solutions [6]. Imidazole itself is usually less protective than its derivatives. So, according to polarization measurements, the protective efficiency of imidazole with respect to Al at a concentration of $18 \cdot 10^{-5}$ M in a 0.5 M HCl solution is 70.7%, and that of 2-methyl imidazole under the same conditions is 76% [6]. The protective efficiency of imidazole with respect to carbon steel in a 0.5 M H_2SO_4 solution at a concentration of 5 mM is 83% [7], and in a 1 M HCl solution at a 4% concentration it is only 60% [8]. However, imidazole with four phenyl substituents provides significantly more effective protection of steel in 1 M HCl and 0.5 M H_2SO_4 [9, 10]. A detailed review of the inhibitory ability of nitrogen-containing five-membered heterocyclic compounds with respect to metals in mineral acid solutions is given in [11].

A known method for producing imidazole and its derivatives by the G. Debus–B.L. Radzishevsky reaction [12, 13] involves the condensation of dicarbonyl compounds with aldehyde and ammonia, where glyoxal, various 1,2-diketones and ketoaldehydes are used as a dicarbonyl reagent. The reaction proceeds according to the following mechanism:

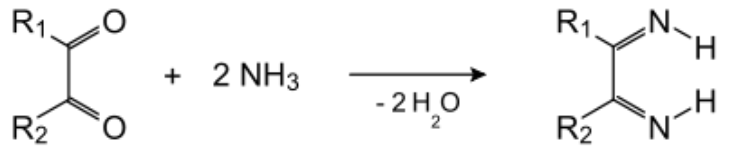

I

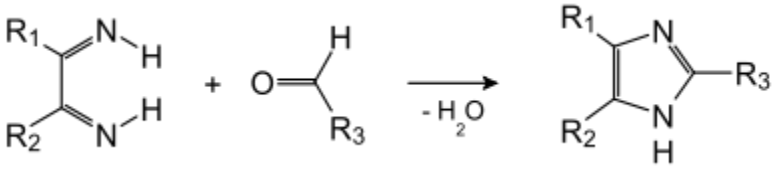

II

At the first stage of the synthesis, if R_1 and R_2 are hydrogen atoms, ammonia undergoes condensation with glyoxal to form a diimine. At the second stage, this diimine reacts with an aldehyde to form an imidazole, if R_3 is a hydrogen atom, or its derivatives, depending on the radical in the aldehyde. In practice, this reaction is not widely used, as it has a low yield and many side products. Nevertheless, the synthesis is characterized by a relatively low cost and availability of raw materials, as well as the simplicity of the technological process.

The purpose of this work is to carry out the G. Debus–B.L. Radzishevsky reaction with the participation of glyoxal, ammonia, and acetaldehyde and evaluate the inhibitory ability of the product obtained in relation to carbon steel in model stratum waters of oil and gas fields containing hydrogen sulfide.

Experimental

For the synthesis of the inhibitor, acetaldehyde with a concentration of 99%, an aqueous solution of glyoxal with a concentration of 40%, and an aqueous solution of ammonia with a concentration of 25% were used. The molar ratio of reagents for the synthesis – ammonia:glyoxal:acetaldehyde – was 2:1:1. Glyoxal is loaded into a four-necked flask equipped with an overhead stirrer, a thermometer and a dropping funnel, and an ammonia solution is slowly introduced through the dropping funnel with stirring. The reaction is accompanied by an exothermic effect, so the flask is cooled with ice water so that the temperature of the reaction mass does not rise above 20°C. After loading the ammonia, the mixture is kept for 30 minutes. Then, acetaldehyde is introduced into the reaction mass in small portions, after which the reaction mass is heated to 50–60°C. The temperature of the reaction mass was raised to 70°C and maintained at this temperature for 3 hours. The reaction mass gradually acquires a yellow color, and then darkens and turns black. With an increase in the synthesis time, as well as an increase in temperature, black plastic agglomerates begin to form in the reaction mass, which indicates the possible polymerization of chemical compounds in the product obtained.

The composition of the product was analyzed by IR spectroscopy and chromato-mass spectrometry. IR Fourier spectrometer Nicolet iS50 FT-IR was used. Experiment parameters: number of sample scans 1500; resolution 4; range 4000–400 cm^{-1}; ATR DTGS detector; beam splitter KBr. Due to the fact that water interferes with the interpretation of the spectrum, the water spectrum was subtracted. The identification of the product composition was carried out on a "Khromatek Kristall 5000.2" chromato-mass spectrometer with subsequent interpretation on the software using the NIST11 mass spectra database.

The product (P) was used as an inhibitor in a concentration of 25–200 mg/L.

Corrosion tests (24 h duration) and electrochemical measurements were carried out at room temperature on St3 carbon steel of composition, wt.%: C, 0.2; Mn, 0.5; Si, 0.15; P, 0.04; S, 0.05; Cr, 0.30; Ni, 0.20; Cu, 0.20; Fe, 98.36. Model stratum waters NACE and M1 [14], saturated with H_2S (400 mg/L) were used as working solutions. The protective effect of the P was calculated according to the data of gravimetric corrosion tests (1) and polarization measurements (2):

$$Z,\% = \frac{K_0 - K_P}{K_0} \cdot 100 \quad (1)$$

$$Z,\% = \frac{i_0 - i_P}{i_0} \cdot 100 \quad (2)$$

where K_0 (i_0) and K_P (i_P) are the corrosion rates in the absence and in the presence of the P in solutions, respectively. Corrosion current densities were calculated by extrapolating the Tafel sections of the polarization curves to the corrosion potential. Potentiodynamic (0.66 mV/s) polarization measurements were carried out using an IPC-Pro potentiostat (produced at A.N. Frumkin Institute of Physical Chemistry and Electrochemistry, RAS). The

potentials were measured with respect to the saturated silver/silver chloride electrode and were recalculated to the standard hydrogen scale. The counter electrode is a smooth platinum.

Impedance spectra were studied in the frequency range ($\omega/2\pi$) of 10 kHz–0.05 Hz with an alternating voltage amplitude of 10 mV, using an electrochemical measuring complex from Solartron (UK) consisting of a SI 1255 impedance analyzer and a SI 1287 potentiostat. The results of impedance measurements were processed according to the procedure described in [15]. Before the experiments, the working electrodes were ground to grade 6 cleanliness and degreased with acetone.

Results and Discussion

Characteristics of the product obtained

The IR spectrum of the product is shown in Figure 1.

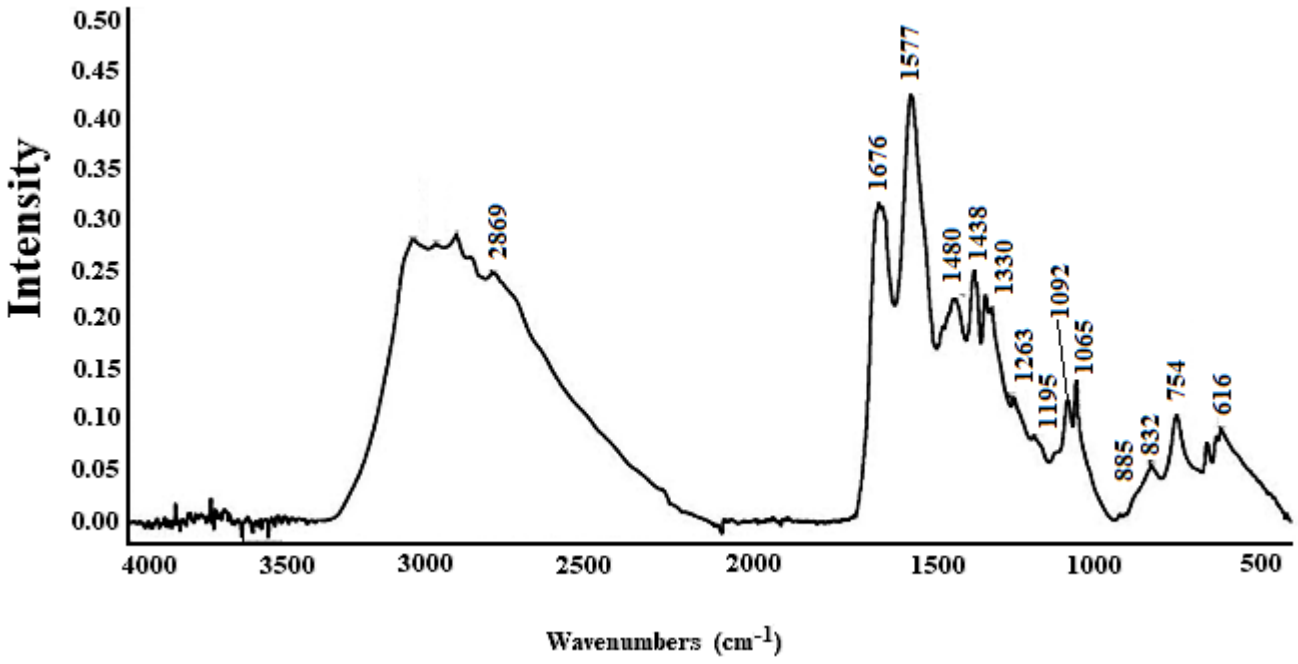

Figure 1. IR spectrum of the product obtained by the reaction of glyoxal, ammonia and acetaldehyde.

Due to the absence of the spectra of imidazole and its derivatives in the library of the spectra of the IR spectrometer, a comparative analysis was carried out according to the literature data of the imidazole spectrum [16]. The data of the comparative analysis of the spectra are given in Table 1.

The chromatogram of the product is shown in Figure 2.

Table 1. Comparison of the data of the reference sample of imidazole with the product obtained as a result of the subtraction of the water spectrum.

Wave numbers, cm^{-1}		Assignment
Reference sample	**Product obtained sample**	
2878	2869	$\nu\ NH_{ass.}$
1670	1676	$\nu\ C{=}N_{cycle}$., $\nu\ C{=}C_{cycle}$
1574	1577	δ NH
1482	1480	δ NH+δ CH
1452	1438	δ NH, δ CH
1330	1330	δ CH
1266	1263	δ CH
1150	1195	δ CH
1100	1092	δ CH
1050	1065	δ CH
888	885	δ CH
836	832	$\gamma\ CH_{oop.}$
754	754	γ CH+γ NH
618	616	ν CNC

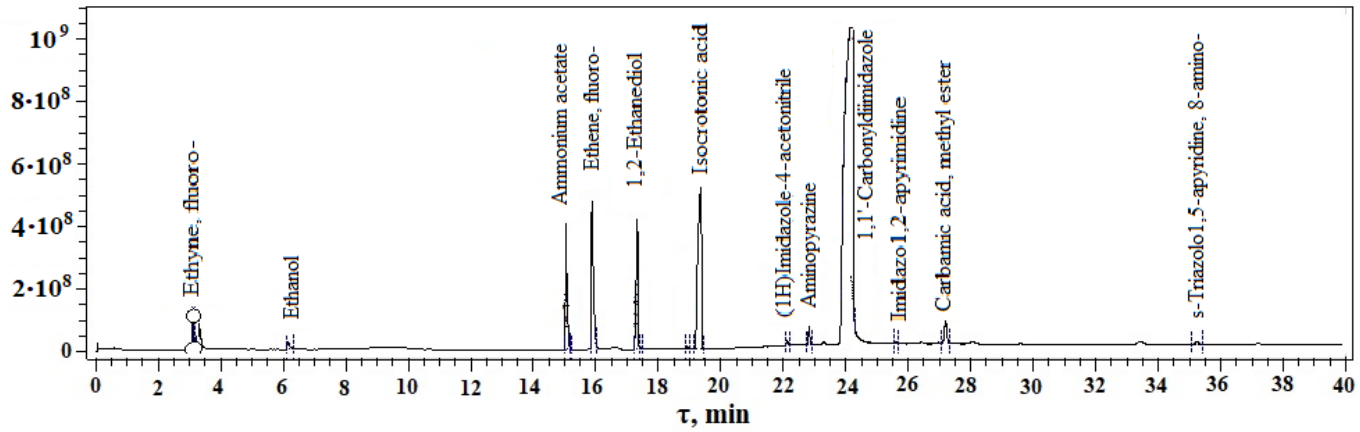

Figure 2. Chromatogram of the product obtained on a chromato-mass spectrometer.

The components of the product are shown in Table 2.

These data indicate the presence of nitrogen-containing compounds including imidazole and its derivatives in the product synthesized.

Table 2. Chemical composition of the product obtained.

No.	Compound Name	Structural formula	Match Probability, %	Peak area, %
1	Ammonium acetate	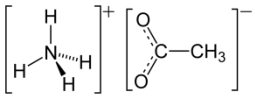	50.15	2.8
2	1,2-Ethanediol		97.01	7.69
3	Formamide	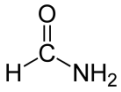	66.26	19.96
4	1*H*-Imidazole		36.81	51.63
5	1*H*-Imidazole, 2-methyl-	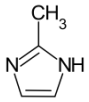	66.45	0.18
6	1,1′-Carbonyldiimidazole	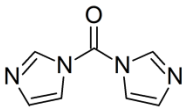	50.71	51.63

Electrochemical and corrosion studies

Figure 3 shows the polarization curves measured in NACE medium+400 mg/L H_2S in the absence and in the presence of the P, and Table 3 shows the kinetic parameters and protective effectiveness calculated on their base. Similar results obtained in M1 medium + 400 mg/L H_2S for the product under study are shown in Figure 4 and in Table 4.

As can be seen from Figure 3 and Table 3, the P slows down both partial electrode reactions in the NACE medium with a protective effect of 83% at concentrations of 100 and 200 mg/L, but the shift of the corrosion potential in the positive direction indicates the predominance of anodic inhibition. In the M1 medium in the presence of the P, the anodic process is slowed down and the cathodic process is facilitated, while E_{cor} is shifted in the positive direction (Figure 4).

Table 4 shows that the product obtained causes an insignificant protective effect at concentrations of 25–100 mg/L, and only at 200 mg/L the *Z* value increases up to 98% according to polarization measurements.

According to gravimetric studies (Table 5), the protective effect of the P increases with an increase in its concentration in both studied media, but the *Z* values were found to be lower than those calculated from the polarization measurements. The discrepancy is obviously due to the different duration of exposure of the electrodes to the solution.

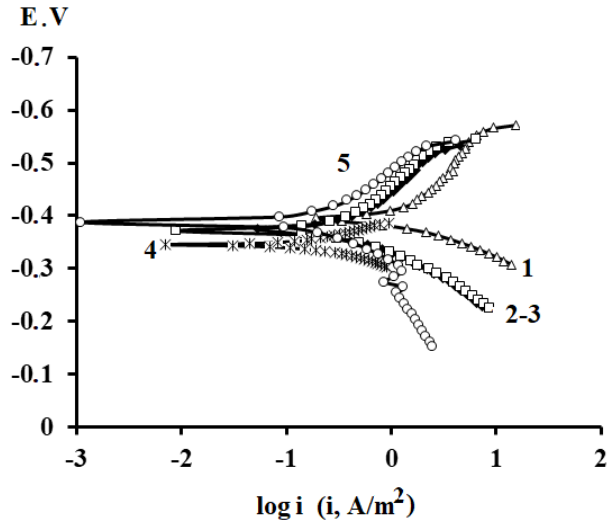

Figure 3. Potentiodynamic polarization curves measured on a steel electrode in NACE medium+400 mg/L H_2S in the absence (1) and in the presence of the P, mg/L: 1 – 25, 2 – 50, 3 – 100, 4 – 200.

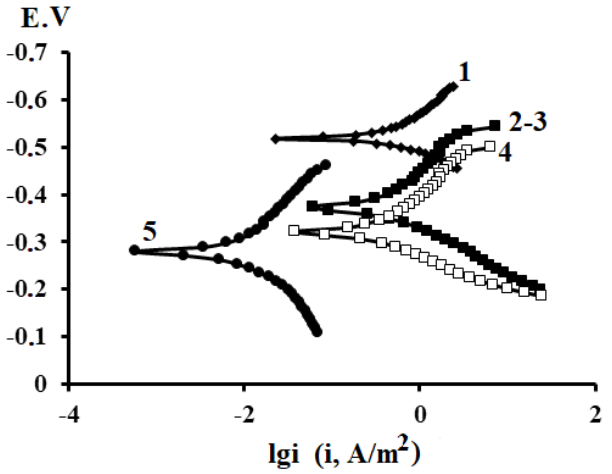

Figure 4. Potentiodynamic polarization curves measured on a steel electrode in M1 medium+400 mg/L H_2S in the absence (1) and in the presence of the P, mg/L: 1 – 25, 2 – 50, 3 – 100, 4 – 200.

Table 3. Kinetic parameters of the St3 steel electrode in NACE+400 mg/L H_2S solution in the absence and in the presence of the P and its protective efficiency.

c_P, mg/L	$-E_{corr}$, V	b_c, V	b_a, V	i_{corr}, A/m^2	Z, %
Absent	0.40	0.14	0.070	0.89	–
25	0.37	0.14	0.070	0.25	72
50	0.37	0.14	0.070	0.25	72
100	0.34	0.12	0.070	0.15	83
200	0.39	0.12	0.090	0.15	83

Table 4. Kinetic parameters of the St3 steel electrode in M1 + 400 mg/L H_2S solution in the absence and in the presence of the P and its protective efficiency.

c_P, mg/L	$-E_{corr}$, V	b_c, V	b_a, V	i_{corr}, A/m^2	Z, %
Absent	0.52	0.16	0,050	0.33	–
25	0.37	0.16	0.050	0.22	33
50	0.38	0.16	0.050	0.22	33
100	0.31	0.16	0.070	0.21	36
200	0.28	0.16	0.070	0.005	98

Table 5. Results of gravimetric tests of St3 steel in NACE and M1 media containing 400 mg/L H_2S and the protective effect of the P (Z,%).

Medium	c_P, mg/L	K, g/(m^2·h)	Z, %
M1	0	0.3122	–
	25	0.1890	39
	50	0.1710	45
	100	0.1471	53
	200	0.1226	61
NACE	0	0.4044	–
	25	0.2585	37
	50	0.1650	59
	100	0.1428	65
	200	0.1186	71

Impedance measurements

The data of impedance measurements at the corrosion potential of the steel electrode confirm the protective effectiveness of the product obtained. Figures 5 and 6 show impedance hodographs of the steel electrode in the media under study. The hodographs are arcs, the radius of which increases with the introduction of the P into the solution and an increase in its concentration, indicating an increase in the total resistance in the system and a decrease in the corrosion rate.

The hodographs are processed in accordance with the equivalent circuit used earlier in [15] and shown in Figure 7. This circuit satisfactorily describes the experimental impedance spectra in the media under study. This follows from the satisfactory agreement between the experimental data and those calculated using the circuit (Figures 5 and 6).

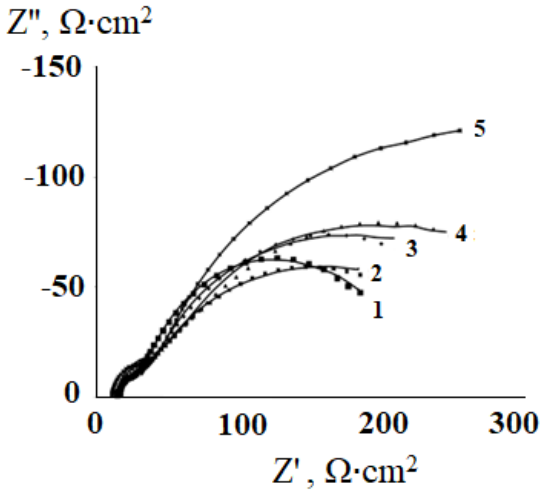

Figure 5. Nyquist diagram of steel electrode in NACE+400 mg/L H_2S solution at corrosion potential in the absence (1) and in the presence of P, mg/L: 2 – 25; 3 – 50; 4 – 100; 5 – 200. The dots correspond to the experimental data, whereas the solid lines correspond to the impedance spectra fitted using the equivalent circuit.

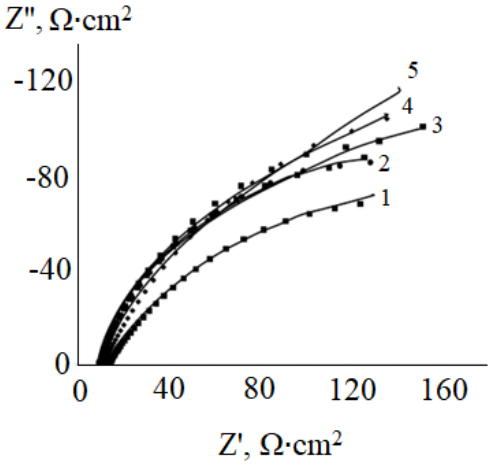

Figure 6. Nyquist diagram of steel electrode in M1+400 mg/L H_2S solution at E_{corr} in the absence (1) and presence of P, mg/L: 2 – 25; 3 – 50; 4 – 100; 5 – 200. The dots correspond to the experimental data, whereas the solid lines correspond to the impedance spectra fitted using the equivalent circuit.

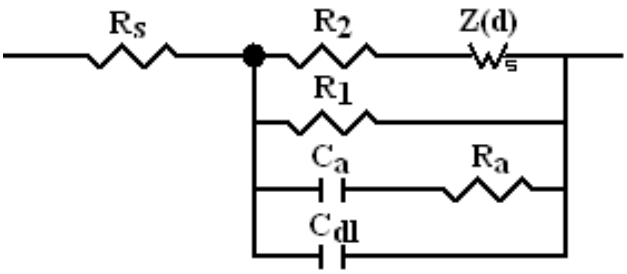

Figure 7. Equivalent circuit simulating the behavior of a steel electrode in test solutions.

Tables 6 and 7 show the numerical values of the equivalent circuit elements in the solutions studied at the corrosion potential without and with tested P concentrations. According to the data presented, in the NACE medium, an increase in the charge transfer resistance in the anodic (R_1) and cathodic (R_2) reactions is observed with an increase in the P concentration (Table 6). This agrees with the data of polarization measurements, indicating a slowdown of both partial electrode reactions in the presence of the product obtained (Figure 3). The value of R_2 is much less than the mass transfer resistance R_D, *i.e.* the reduction of the depolarizer proceeds with a predominance of diffusion restrictions. R_D increases with an increase in the P concentration. The parameter p, corresponding to the generalized final diffusion impedance $Z_D = R_D \text{th}(j\omega\tau)^p/(j\omega\tau)^p$, where $0 < p < 1$, retains a value close to 0.6 at all the P concentrations.

Table 6. Numerical values of elements of the equivalent circuit at E_{corr} of the steel electrode in NACE+400 mg/L H_2S solution without and with tested concentrations of the P.

Element	P concentration, mg/L				
	Background	**25**	**50**	**100**	**200**
R_s, Ω·cm^2	14.5	16.0	15.6	13.4	10.8
R_2, Ω·cm^2	16.2	17.2	18.8	23.6	25.5
R_D, Ω·cm^2	2915	2187	4587	5638	6483
τ_d, s	14.1	26.9	46.8	88.4	90.1
p_d	0.70	0.57	0.63	0.55	0.63
R_1, Ω·cm^2	213	259	285	360	468
C_a, μF/cm^2	28.7	41.6	36.7	23.5	30.5
R_a, Ω·cm^2	12.2	1.9	1.9	4.0	2.4
C_{dl}, μF/cm^2	51.2	17.3	14.1	4.7	6.5

Table 7. Numerical values of elements of the equivalent circuit at E_{corr} of the steel electrode in M1+400 mg/L H_2S solution without and with tested concentrations of the P.

Element	P concentration, mg/L				
	Background	**25**	**50**	**100**	**200**
R_s, Ω·cm^2	12.2	8.6	8.3	8.5	8.3
R_2, Ω·cm^2	2.1	1.4	2.7	2.1	3.3
R_D, Ω·cm^2	1164	1287	1447	1481	1292
τ_d, s	36.8	28.0	24.6	24.1	26.8

Element	P concentration, mg/L				
	Background	**25**	**50**	**100**	**200**
p_d	0.63	0.71	0.73	0.73	0.71
R_1, Ω·cm^2	256	261	257	282	362
C_a, μF/cm^2	215.7	23.7	1310.2	1418.9	152.7
R_a, Ω·cm^2	7.9	5.6	3.3	3.4	3.3
C_{dl}, μF/cm^2	38.4	15.3	11.7	9.4	9.7

The value of p within the specified limits is observed in the case of non-conservation of the number of diffusing particles in the diffusion layer or when some particles are delayed for a relatively long time at certain points of the diffusion layer [17]. This is quite likely due to the different nature of the substances contained in the P.

In the M1 medium, the charge transfer resistance in the anodic reaction R_1 increases with an increase in the P concentration, but the R_2 value remains almost unchanged. This corresponds to the data of polarization measurements, indicating a slowdown in the anode process (Figure 4). The mass transfer resistance R_D significantly exceeds the value of R_2, as in the NACE medium, and tends to increase with increasing concentration of the P. The parameter p has a value within the above limits, apparently for the same reason as in the NACE medium, retaining a practically unchanged value close to 0.7 at all the P concentrations.

The capacitance of the electric double layer C_{dl} decreases with an increase in the P concentration in both media, which indicates its adsorption and allows to calculate the electrode surface coverage Θ with the components of the product obtained using the formula [18]:

$$\Theta = \frac{C_0 - C}{C_0 - C_1}, \quad (3)$$

where C_0, C and C_1 are the capacitances of the electric double layer in the solution without addition of P, with that and with the maximum coverage of the electrode surface with the adsorbed particles, respectively. The value of C_1 is calculated graphically on the basis of the rectilinear dependence $C_{dl}=C_{dl}(1/c_{Inh})$ and is equal to the segment cut off on the y-axis [15]. In NACE solution C_1=3.5 μF/cm^2, in M1 medium C_1=8.0 μF/cm^2. The calculated values of Θ are shown in Table 8.

To select an isotherm corresponding to the data given in Table 8, it was checked their correspondence to the Temkin isotherm $Bc=\exp(f\cdot\Theta)$, the Frumkin isotherm $Bc=[\Theta/(1-\Theta)]\exp(-2a\Theta)$, and the Langmuir isotherm $c/\Theta=1/B+c$, where f is the factor of the energy inhomogeneity of the surface, B is the constant of adsorption equilibrium, a is the attraction constant characterizing the interaction between adsorbed particles, c is an inhibitor

concentration. For this, the graphic dependences of Θ *vs.* (log *c*), corresponding to the Temkin and Frumkin isotherms, and *c*/Θ *vs. c* corresponding to the Langmuir isotherm were considered (Figure 8).

Table 8. Influence of the P concentration on the surface coverage of steel in the NACE and M1 media containing 400 mg/L H_2S.

c_P, mg/L	25	50	100	200
Θ in NACE medium	0.71	0.78	0.97	0.94
Θ in M1 medium	0.76	0.88	0.95	0.94

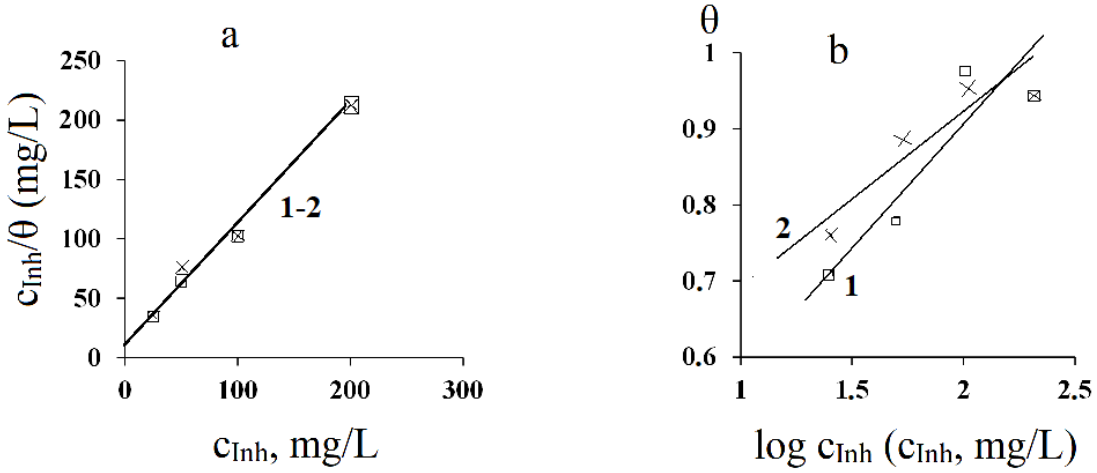

Figure 8. Adsorption isotherms for St3 steel in NACE+400 mg/L H_2S (1) and M1+400 mg/L H_2S (2) solutions.

As can be seen from Figure 8, the best fit to the linear dependence is observed for the Langmuir isotherm, with the experimental points corresponding to the NACE and M1 media falling on one straight line. In this case, the segment cut off on the vertical axis of Figure 8a allows to calculate the adsorption equilibrium constant *B* (*B*=0.1 L/mg), which corresponds to both media. Knowing the constant *B*, it is possible to calculate the value of free adsorption energy $-\Delta G^0_{ads}$ according to the equation:

$$-\Delta G^0_{ads} = RT \ln\left(B \cdot 10^6\right),$$

where 10^6 is the concentration of water in the solution, mg/L.

The value $-\Delta G^0_{ads}$ at a temperature of 298 K in the media under study is 28.5 kJ/mol. It can be assumed that there is a physical adsorption of inhibitory components with a certain amount of chemisorption.

Conclusions

The G. Debus–B.L. Radzishevsky reaction with the participation of glyoxal, ammonia, and acetaldehyde performed in laboratory made it possible to obtain a mixture of nitrogen-containing products identified by chromatography-mass spectrometry and IR spectroscopy.

The inhibitory ability of the product obtained with respect to hydrogen sulfide corrosion of carbon steel in model stratum waters of oil and gas fields was studied by electrochemical and gravimetric methods.

According to gravimetry, the protective effect of the product at a concentration of 200 mg/L is about 60% in the NACE medium and 70% in the M1 medium containing 400 mg/L H_2S. Polarization measurements show higher Z values equal to 83 and 98%, respectively.

The deceleration of corrosion is due to the inhibition of both partial electrode reactions in the NACE medium and the anodic reaction in the M1 medium due to the adsorption of the product components on the metal in accordance with the Langmuir isotherm. The calculated value of the free adsorption energy, equal to –28.5 kJ/mol, indicates the physical adsorption of inhibitory components with a certain amount of chemisorption.

Acknowledgment

The results were obtained using the equipment of the Center for Collective Use of Scientific Equipment of TSU named after G.R. Derzhavin. This work was supported by the Ministry of Science and Higher Education of the Russian Federation in the frame work of agreement No. 075-15-2021-709 (unique project identifier RF-2296.61321X0037).

The team of authors expresses their gratitude to Andrey Knyazev, director of NOVOKHIM (Novochem), for providing glyoxal for this study.

References

1. T. Yanardag, S. Özbay, S. Dinçer and A.A. Aksut, Corrosion Inhibition Efficiency of Benzimidazole and Benzimidazole Derivatives for Zinc, Copper and Brass, *Asian J. Chem*., 2012, **24**, 47–52.
2. T. Yan, S. Zhang, L. Feng, Y. Qiang, L. Lu, D. Fu, Y. Wen, J. Chen, W. Li and B. Tan, Investigation of imidazole derivatives as corrosion inhibitors of copper in sulfuric acid: Combination of experimental and theoretical researches, *J. Taiwan Inst. Chem. Eng*., 2020, **106**, 118–129. doi: 10.1016/j.jtice.2019.10.014
3. Y. Qiang, S. Zhang, L. Guo, X. Zheng, B. Xiang and S. Chen, Experimental and theoretical studies of four allyl imidazoliumbased ionic liquids as green inhibitors for copper corrosion in sulfuric acid, *Corros. Sci*., 2017, **119**, 68–78. doi: 10.1016/j.corsci.2017.02.021
4. R. Gasparac and E. Stupnisek-Lisac, Corrosion Protection on Copper by Imidazole and its Derivatives, *Corrosion*, 1999, **55**, no. 11, 1031–1039. doi: 10.5006/1.3283940

5. W.J. Lee, Inhibiting effects of imidazole on copper corrosion in 1 M HNO_3 solution, *Mater. Sci. Eng. A*, 2003, **348**, no. 1–2, 217–226. doi: 10.1016/S0921-5093(02)00734-7
6. M.N. El-Haddad and A.S. Fouda, Electroanalytical, quantum and surface characterization studies on imidazole derivatives as corrosion inhibitors for aluminum in acidic media, *J. Mol. Liq*., 2015, **209**, 480–486. doi: 10.1016/j.molliq.2015.06.005
7. M. Abdallah, I. Zaafarany, K.S. Khairou and M. Sobhi, Inhibition of Carbon Steel Corrosion by Iron(III) and Imidazole in Sulfuric Acid, *Int. J. Electrochem. Sci*., 2012, **7**, no. 2,1564–1579.
8. S.A. Mangai and S. Ravi, Comparative Corrosion Inhibition Effect of Imidazole Compounds and of *Trichodesma indicum* (Linn) R. Br. on C38 Steel in 1 M HCl Medium, *J. Chem*., 2013, **2013**, 527286. doi: 10.1155/2013/527286
9. M. Ouakki, M. Galai, M. Rbaa, A.S. Abousalem, B. Lakhrissi, M. Ebn Touhami and M. Cherkaoui, Electrochemical, thermodynamic and theoretical studies of some imidazole derivatives compounds as acid corrosion inhibitors for mild steel, *J. Mol. Liq*., 2020, **319**, 114063. doi: 10.1016/j.molliq.2020.114063
10. M. Ouakki, M. Galai, M. Rbaa, A.S. Abousalem, B. Lakhrissi, E.H. Rifi and M. Cherkaoui, Quantum chemical and experimental evaluation of the inhibitory action of two imidazole derivatives on mild steel corrosion in sulphuric acid medium, *Heliyon*, 2019, **5**, no. 11, e02759. doi: 10.1016/j.heliyon.2019.e02759
11. Ya.G. Avdeev and Yu.I. Kuznetsov, Nitrogen-containing five-membered heterocyclic compounds as corrosion inhibitors for metals in solutions of mineral acids – An overview, *Int. J. Corros. Scale Inhib*., 2021, **10**, no. 2, 480–540. doi: 10.17675/2305-6894-2020-10-2-2
12. A.F. Pozharsky, *Teoreticheskie osnovy khimii geterotsyklov (Theoretical foundations of the chemistry of heterocycles)*, Moscow, Khimiya, 1985, 279 (in Russian).
13. M. Bouchakour, M. Daaou and N. Duguet, Synthesis of Imidazoles from Fatty 1,2-Diketones, *Eur. J. Org. Chem*., 2021, **2021**, no. 11, 1647–1652. doi: 10.1002/ejoc.202100053
14. L.E. Tsygankova, A.A. Uryadnikov, A.E. Abramov and T.V. Semenyuk, Inhibiting compositions against hydrogen sulfide corrosion of carbon steel, *Int. J. Corros. Scale Inhib*., 2022, **11**, no. 1, 102–110. doi: 10.17675/2305-6894-2021-11-1-5 .
15. L.E. Tsygankova, V.A. Bryksina, A.A. Uryadnikov and A.E. Abramov, Protective efficiency of expired drug against acid corrosion of carbon steel, *Int. J. Corros. Scale Inhib*., 2022, **11**, no. 2, 564–576. doi: 10.17675/2305-6894-2022-11-2-7
16. N.U. Mulloev, Z.Z. Islomov, M. Fayzieva, R. Safarova and J. Yusupova, IK-spektry rodstvennykh geterotsyklicheskikh soedinenii (IR spectra of related heterocyclic compounds), *Proceedings of the Academy of Sciences of the Republic of Tajikistan. Department of physical and mathematical, chemical, geological and technical sciences*, 2015, no. 3, 160 (in Russian).

17. J. Bisquert and A. Compte, Theory of the electrochemical impedance of anomalous diffusion, *J. Electroanal. Chem*., 2001, **499**, no. 1, 112–120. doi: 10.1016/S0022-0728(00)00497-6
18. B.B. Damaskin, O.A. Petriy and V.V. Batrakov, *Adsorption of organic compounds on electrodes*, Moscow, Nauka, 1968, 334 (in Russian).

♦ ♦ ♦